

Supporting Information

Li et al. 10.1073/pnas.0901765106

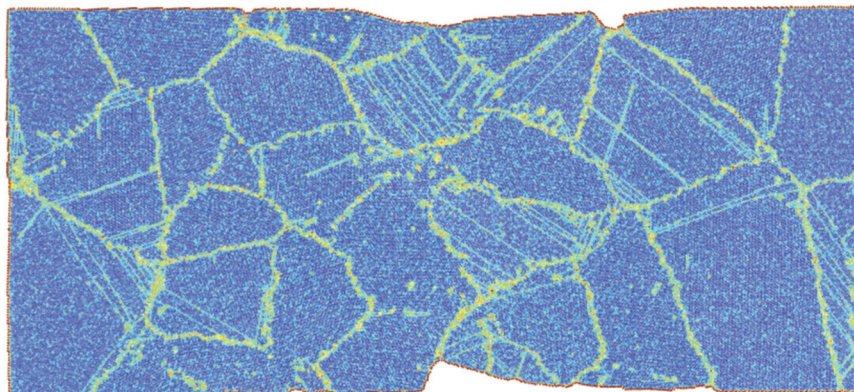


Fig. S1. Potential energy mappings of different configurations shown in Fig. 1. (A) Initial configuration at 300 K. (B–D) Final configurations at 300, 500, and 700 K, respectively. GBs have high energy because of their highly disordered atomic structure. (Scale bar, 5 nm).

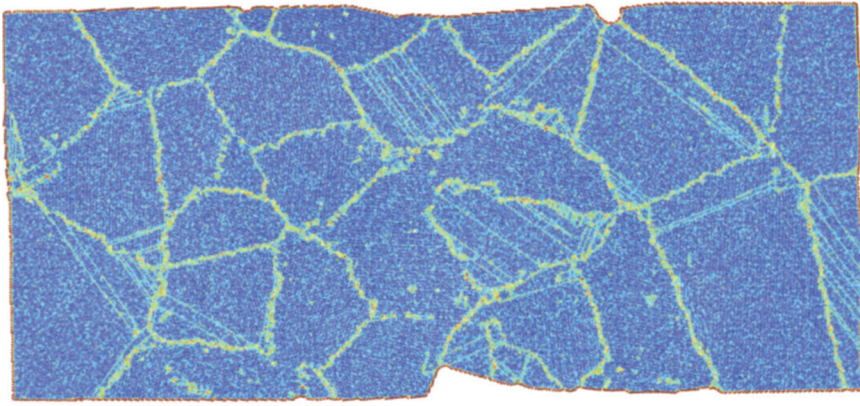


Fig. S1 (continued).

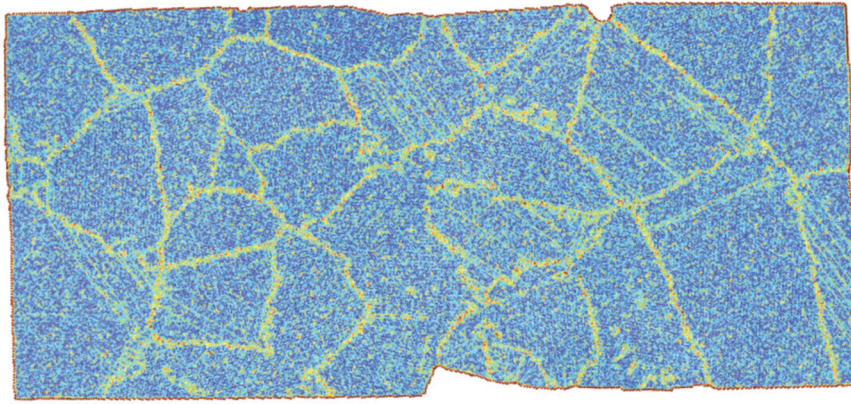


Fig. S1 (continued).

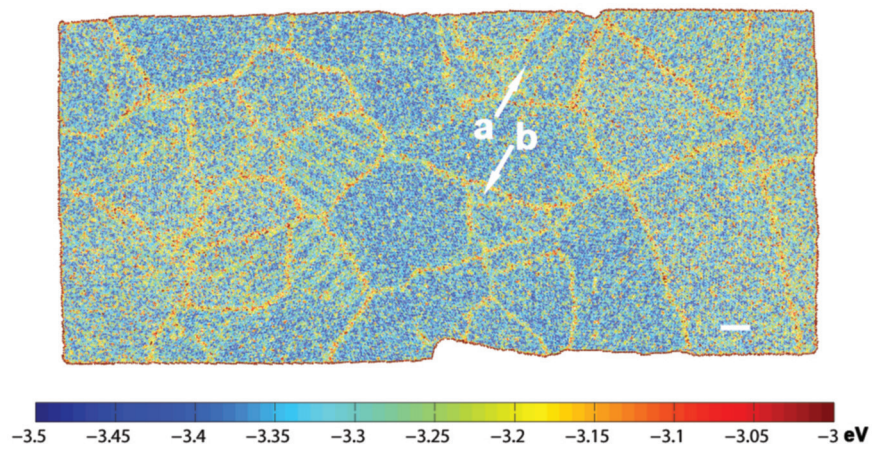


Fig. S1 (continued).

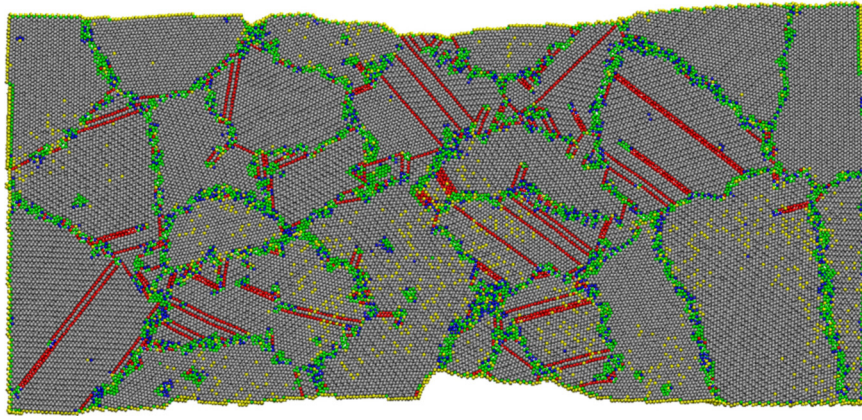


Fig. 52. Snapshot configurations of the $d = 10$ nm sample right before and after strain recovery at different temperatures. (A) Initial configuration at 300 K. (B–D) Final configurations at 300, 500, and 700 K, respectively. Several grains incorporate and then grow during annealing. (Scale bar, 5 nm).

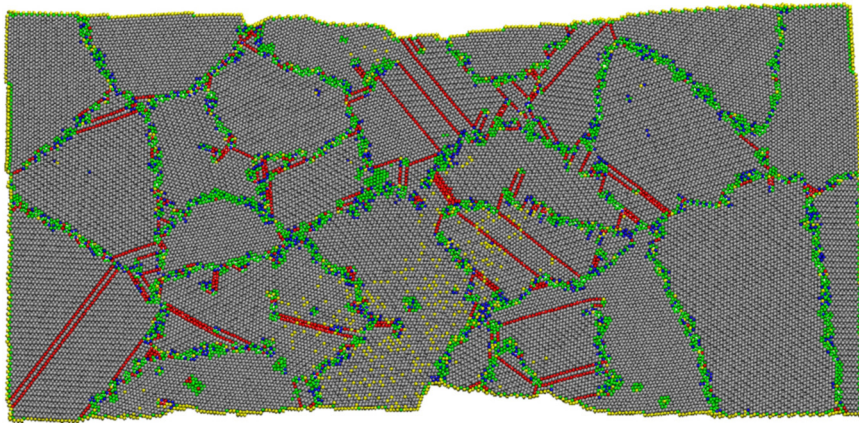


Fig. S2 (continued).

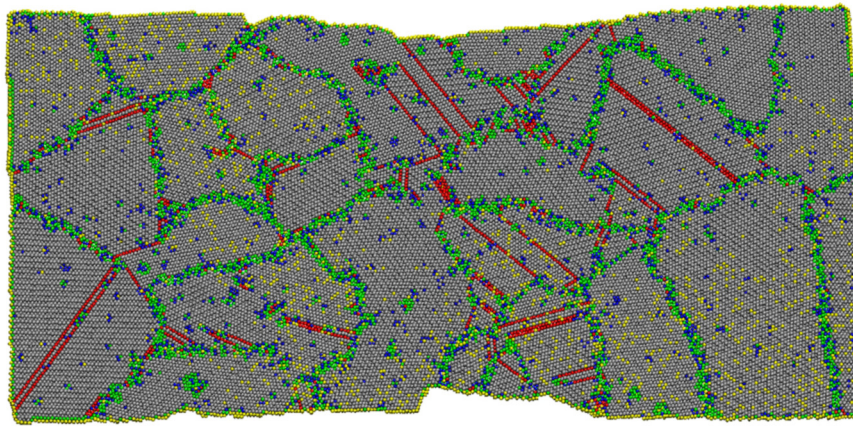


Fig. S2 (continued).

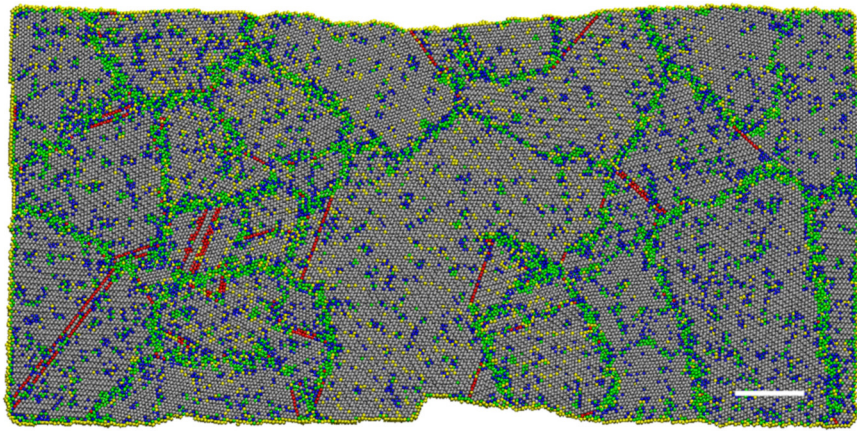


Fig. S2 (continued).

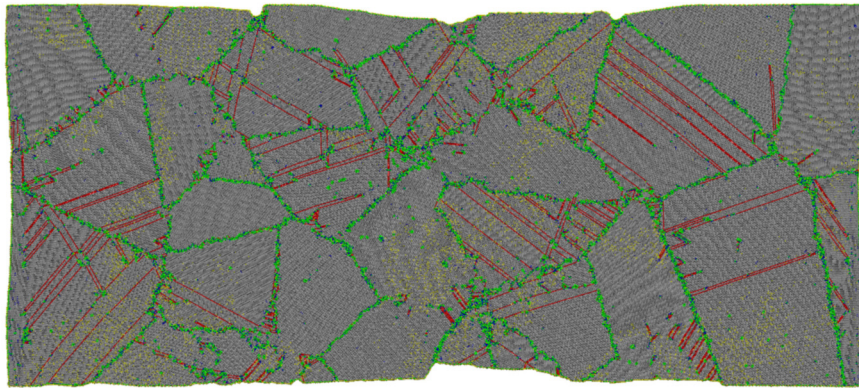


Fig. S3. Snapshot configurations of the $d = 30$ nm sample right before and after strain recovery at different temperatures. (A) Initial configuration at 300 K. (B–D) Final configurations at 300, 500, and 700 K, respectively. Some grains grow during annealing. A few small grains form at high temperature, which implies a dynamic recrystallization process during annealing. (Scale bar, 5 nm).

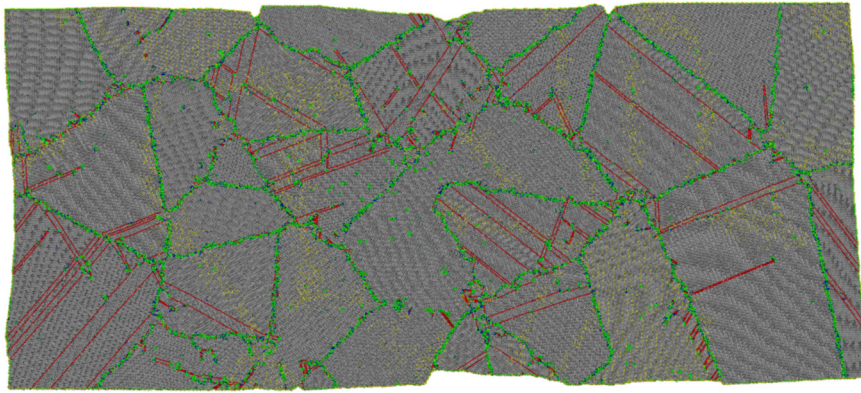


Fig. S3 (continued).

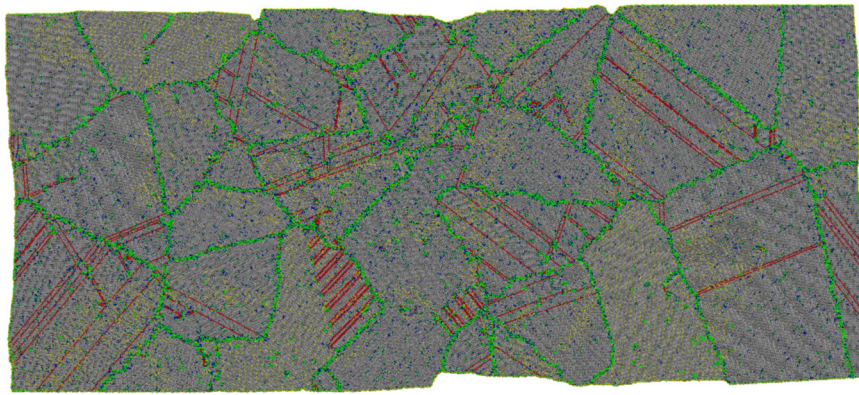


Fig. S3 (continued).

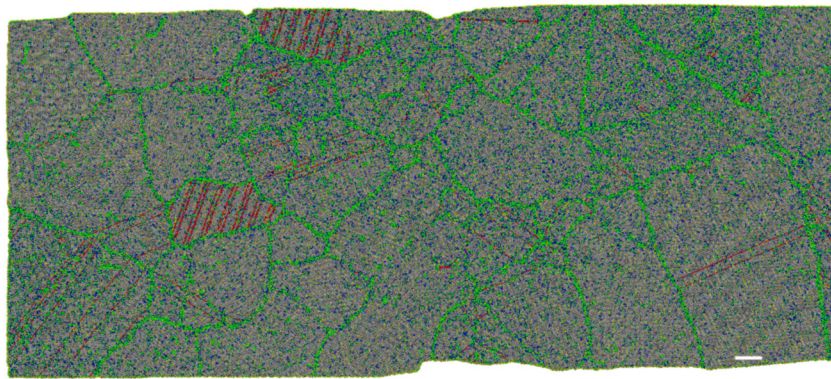


Fig. S3 (continued).

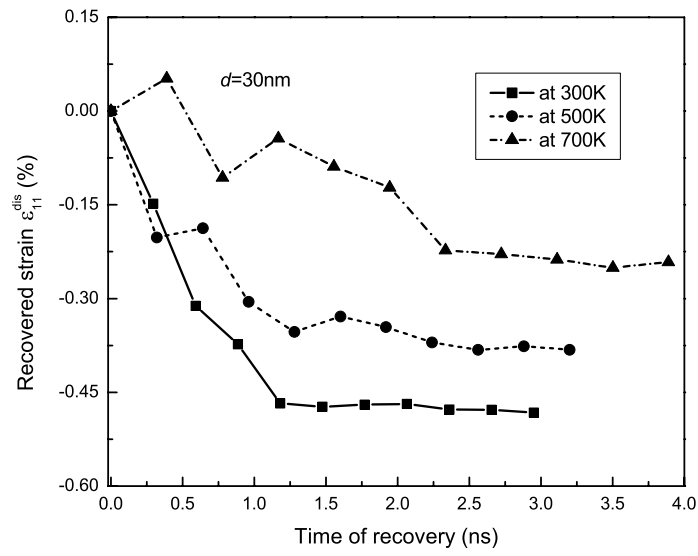


Fig. S4 (continued).

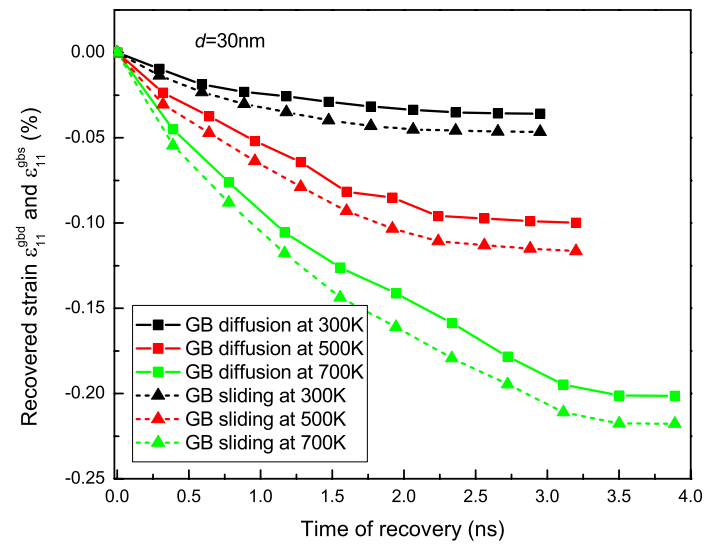


Fig. S4 (continued).

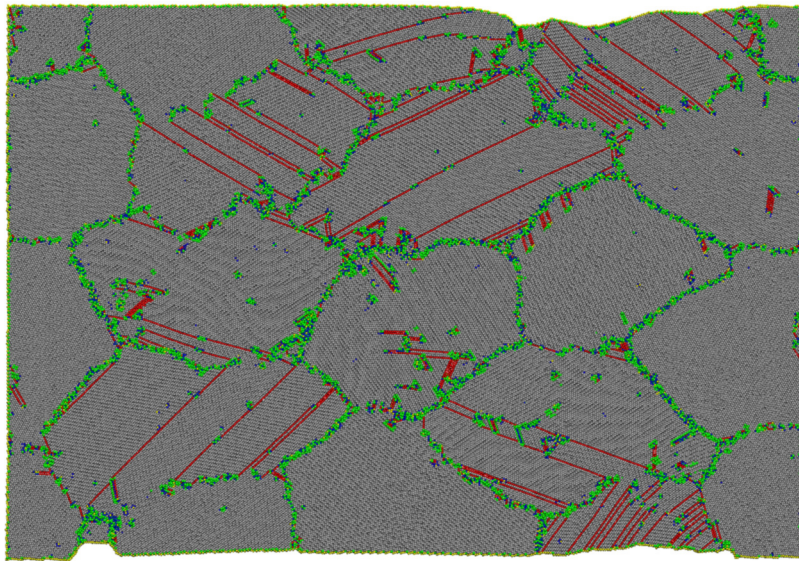


Fig. S5. Snapshot configurations of the "real" sample with a mean grain size of $d = 20$ nm right before and after strain recovery stage at different temperatures. (A) Initial configuration at 300 K. (B–D) Final configurations at 300, 500, and 700 K. Some grains distinctly change their shape during annealing. It is obviously observed that the dynamic recrystallization occurs during annealing. (Scale bar, 5 nm).

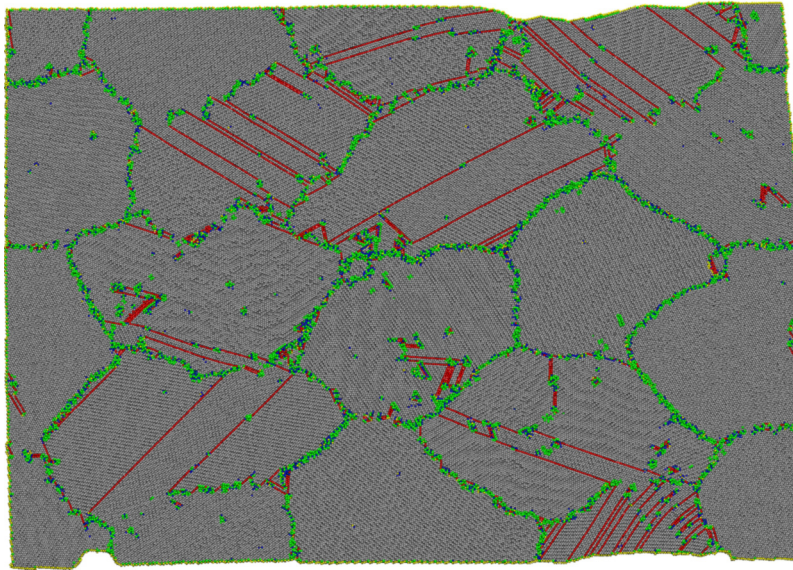


Fig. S5 (continued).

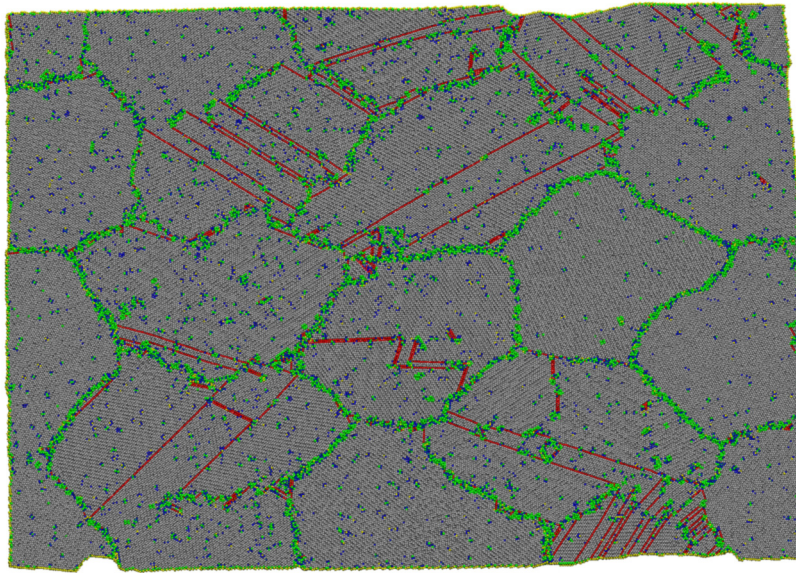


Fig. S5 (continued).

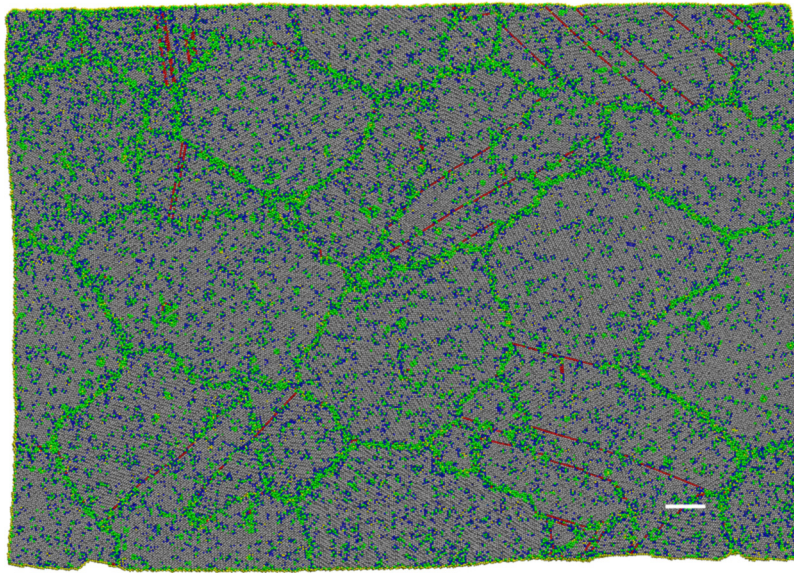


Fig. S5 (continued).

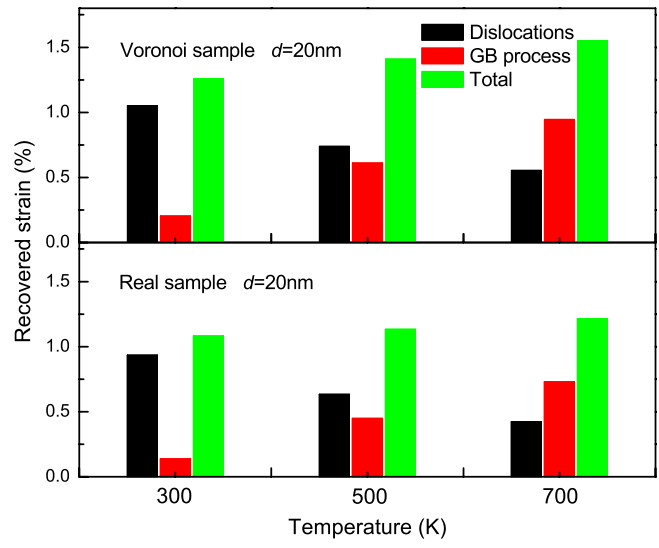
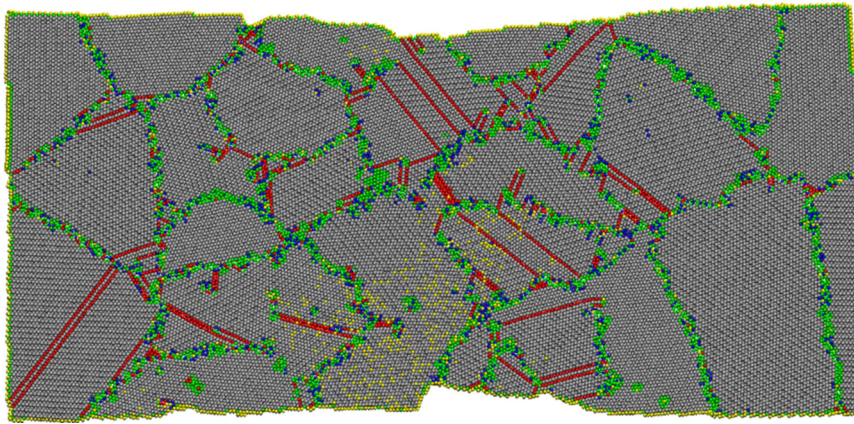
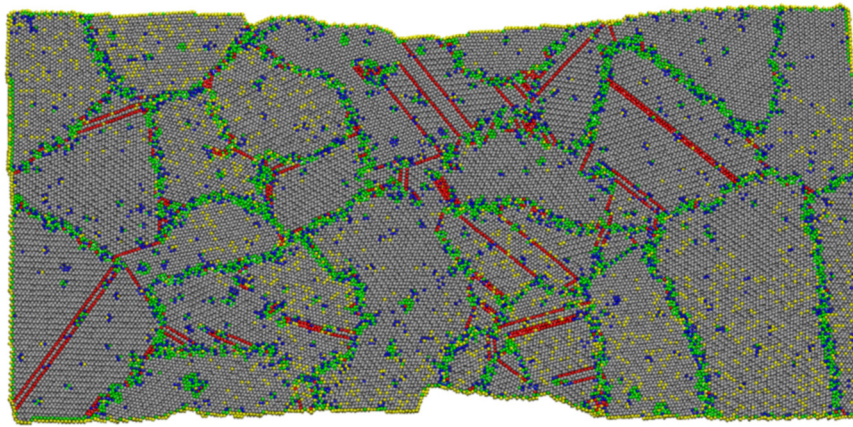


Fig. S6. Fractional strains due to GB- and dislocation-mediated mechanisms in the “Voronoi” and “real” samples at different temperatures.



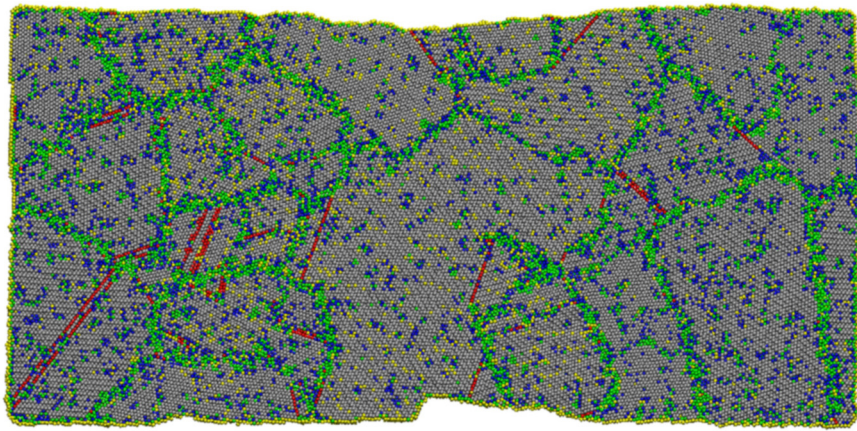
Movie S1. Movies S1–S9 show the plastic strain recovery in nanocrystalline (nc) Al samples with mean grain sizes of $d = 10, 20,$ and 30 nm at different recovery temperatures of $300, 500,$ and 700 K, respectively. All movies include three stages: loading, unloading, and strain recovery. At lower temperatures/larger grain sizes, dislocation activities tend to dominate the plastic strain recovery. In addition, deformation twinning occurs due to interplay of adjacent partial dislocations. At higher temperatures/smaller grain sizes, GB sliding and GB diffusion become dominant in the recovery process. GB diffusion is activated by stress-assisted migration or flow of vacancies along GBs. GB sliding accompanies GB diffusion as an accommodation process. It is noted that some grains are formed at high temperatures. Such phenomena indicate a dynamic recrystallization process in nc Al. Movie S1 is an animation of plastic deformation in nc Al with a mean grain size of $d = 10$ nm. The sample is loaded (to a strain of 9.3%) and unloaded at room temperature, followed by annealing at 300 K.

[Movie S1 \(AVI\)](#)



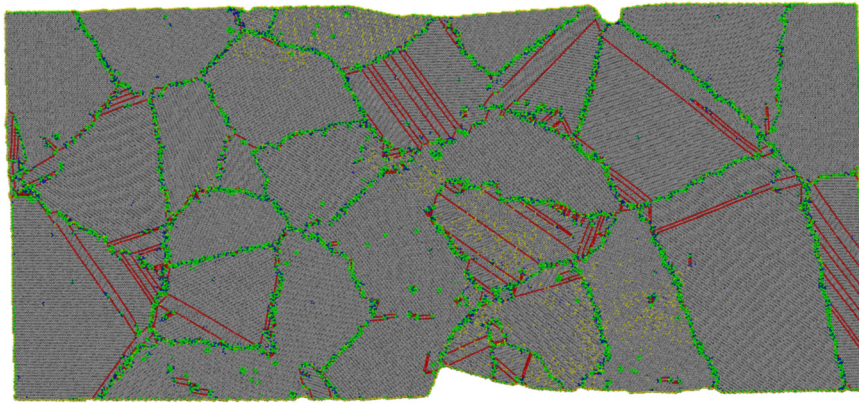
Movie S2. Animation of plastic deformation in nc Al with a mean grain size of $d = 10$ nm. The sample is loaded (to a strain of 9.3%) and unloaded at room temperature, followed by annealing at 500 K.

[Movie S2 \(AVI\)](#)



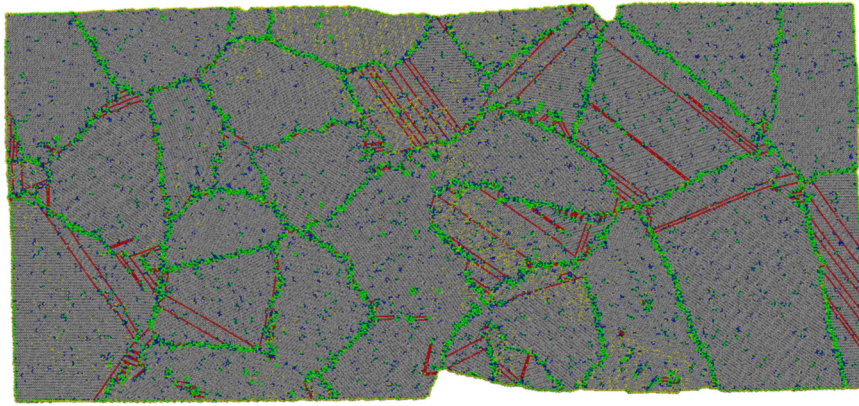
Movie S3. Animation of plastic deformation in nc Al with a mean grain size of $d = 10$ nm. The sample is loaded (to a strain of 9.3%) and unloaded at room temperature, followed by annealing at 700 K.

[Movie S3 \(AVI\)](#)



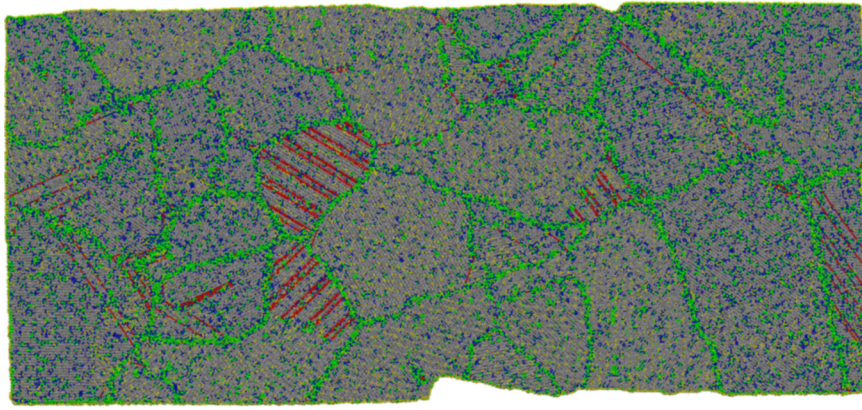
Movie S4. Animation of plastic deformation in nc Al with a mean grain size of $d = 20$ nm. The sample is loaded (to a strain of 9.3%) and unloaded at room temperature, followed by annealing at 300 K.

[Movie S4 \(AVI\)](#)



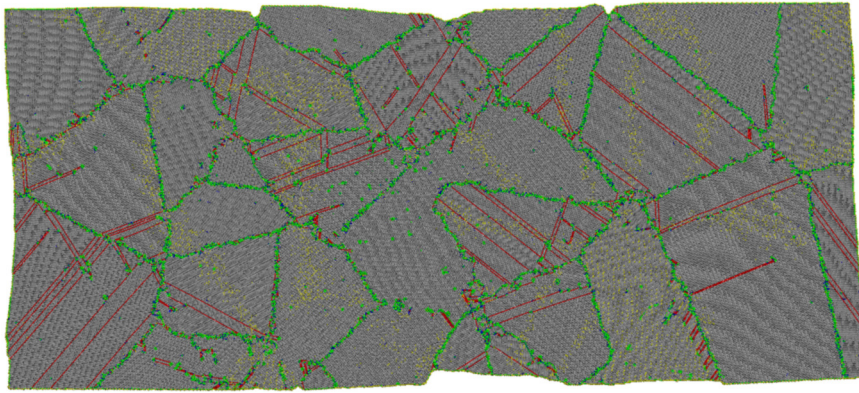
Movie S5. Animation of plastic deformation in nc Al with a mean grain size of $d = 20$ nm. The sample is loaded (to a strain of 9.3%) and unloaded at room temperature, followed by annealing at 500 K.

[Movie S5 \(AVI\)](#)



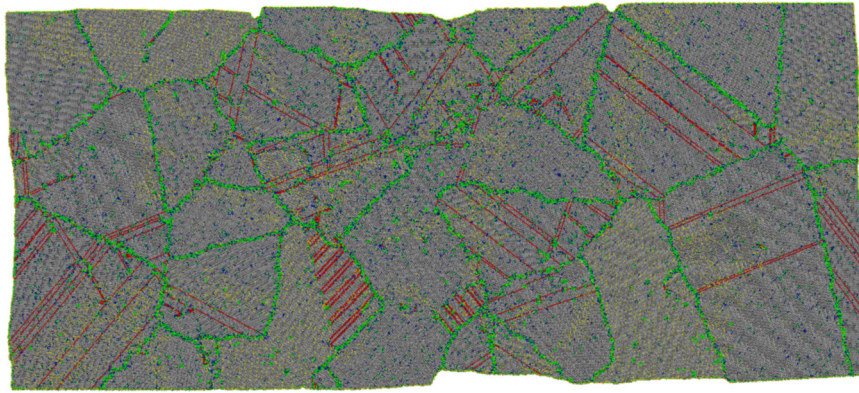
Movie S6. Animation of plastic deformation in nc Al with a mean grain size of $d = 20$ nm. The sample is loaded (to a strain of 9.3%) and unloaded at room temperature, followed by annealing at 700 K.

[Movie S6 \(AVI\)](#)



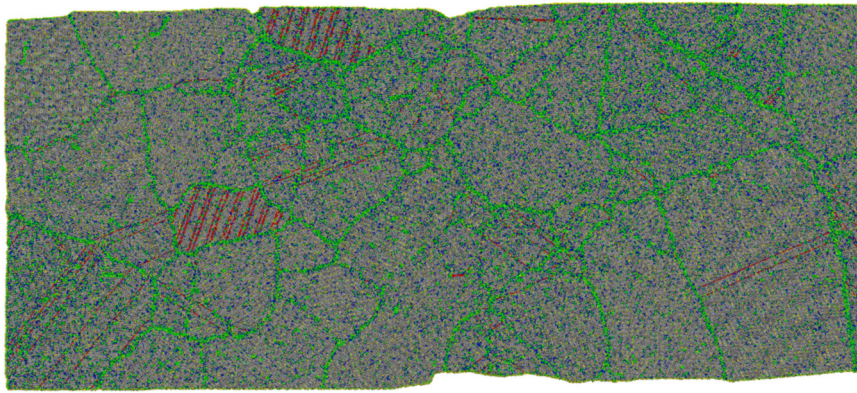
Movie 57. Animation of plastic deformation in nc Al with a mean grain size of $d = 30$ nm. The sample is loaded (to a strain of 9.3%) and unloaded at room temperature, followed by annealing at 300 K.

[Movie 57 \(AVI\)](#)



Movie S8. Animation of plastic deformation in nc Al with a mean grain size of $d = 30$ nm. The sample is loaded (to a strain of 9.3%) and unloaded at room temperature, followed by annealing at 500 K.

[Movie S8 \(AVI\)](#)



Movie S9. Animation of plastic deformation in nc Al with a mean grain size of $d = 30$ nm. The sample is loaded (to a strain of 9.3%) and unloaded at room temperature, followed by annealing at 700 K.

[Movie S9 \(AVI\)](#)